Recent Developments in
Low Cost Stable Structures for Space

Timothy C. Thompson, Cathleen Grastataro, Brian G. Smith
Los Alamos National Laboratory, Los Alamos, NM

Abstract

The Los Alamos National Laboratory (LANL) in partnership with Composite Optics Incorporated (COI) is advancing the development of low cost, lightweight, composite technology for use in spacecraft and stable structures. The use of advanced composites is well developed, but the application of an all-composite tracker structure has never been achieved. This paper investigates the application of composite technology to the design and fabrication of an all-composite spacecraft bus for small satellites, using technology directly applicable to central tracking in a high luminosity environment.

The satellite program Fast On-Orbit Recording of Transient Events (FORTÉ) is the second in a series of satellites to be launched into orbit for the US Department of Energy (DOE). This paper will discuss recent developments in the area of low cost composites, used for either spacecraft or ultra stable applications in high energy physics (HEP) detectors. The use of advanced composites is a relatively new development in the area of HEP. The Superconducting Super Collider (SSC) spawned a new generation of Trackers which made extensive use of graphite fiber reinforced plastic (GFRP) composite systems. LANL has designed a structure employing new fabrication technology. This concept will lower the cost of composite structures to a point that they may now compete with conventional materials. This paper will discuss the design, analysis and proposed fabrication of a small satellite structure. Central tracking structures using advanced materials capable of operating in an adverse environment typical of that found in a high luminosity collider could use identical concepts. LANL designed and analyzed the proposed technology for use on the gamma, electron, and muon (GEM) detector.

This paper will discuss the issues of design, analysis, testing, and fabrication required to deliver the FORTÉ spacecraft applications, and its associated components within a two-year period. Due to the extremely tight time constraints, a novel low-cost solution using GFRP composites was required to achieve the performance goals of the mission. The paper will give the details of material selection, characterization of design allowables, and the approach used in determining the structural geometry that will provide the optimum performance for this mission are presented.

1. Introduction

1.1. Overview

There is currently considerable interest in the use of low cost, small satellites to increase the ratio of payload-to-structure performance for space missions. This technology can be used to significantly reduce the cost of structures proposed for large stable detectors used for Large Hadron Collider (LHC).

A common practice for constructing small spacecraft structures is to use an all-aluminum spacecraft bus. This reduces the payload capacity significantly, however the cost of the aluminum structure has historically been lower than using advanced composites. LANL mission requirements dictate the need for a long term solution which substantially increased the ratio of payload to structural mass while maintaining a low-risk low cost approach. LANL intends to use the concept developed for FORTÉ on future HEP central tracking structures.

1.2. Aluminum vs. Composites

LANL and its industrial partner (COI) have built an all-graphite composite spacecraft structure. Incorporating advanced materials and unique manufacturing techniques, this structure will enable higher fractions of useful payload (as a percentage of total launch weight) to be placed in orbit. The FORTÉ experiment will provide the test bed and space validation for this structure and for other key aspects of these technologies that can be used in other HEP programs. This major technology development will make a significant contribution to the nation's many industrial pursuits that involve advanced performance structures.

Staying close to known designs and well-known materials can go a long way in reducing risk and cost of stable structures as in this case of a spacecraft. The original proposed design was an all-aluminum bolted structure that did not meet the weight target. Composites have a clear advantage in performance over aluminum and are required to meet the mission weight objectives.

2. Spacecraft Configuration

2.1. Design Approach

Several factors influenced the FORTÉ design. The approach used by LANL was to do a sufficient amount of analysis to validate the design concept and to thoroughly test the concept through rigorous testing of the spacecraft. The schedule permitted two design iterations that allowed the Engineering Model (EM) to be thoroughly tested and subsequent changes to be fed back into the final flight hardware that will be constructed in the fall of 1994. The geometry is simple and modular for low cost and improved maintainability and repairability. The configuration selected allowed us to efficiently use the solar array substrate (SAS) panels for shear panels and as a load-bearing member. Finally, materials that are critical to the project's success have already been proven in space.

2.2. Design Considerations

The resulting design drivers for the spacecraft bus are weight, strength, stiffness, and launch vehicle volume. The overall cost, schedule and associated risks with performance, cost, and schedule also have a significant influence on the design.

2.3. Description of Spacecraft and Payload

The FORTÉ spacecraft primary structure consists of 6 major structural components, 3 structural trusses, 3 instrument decks, and 24 SAS panels. The fundamental principles behind this unique spacecraft design are simplicity, modularity and interchangeability, as shown in Figure 1.

The three frame structural trusses are termed the lower, mid and upper cages. The lower and mid cages are identical to each other. Rectangular frame subassemblies comprise the lower and mid cages. The upper cage assembly is constructed using trapezoidal frame subassemblies. Eight frame subassemblies are bonded together to form each of the three octagonal cages, as shown in Figure 2.
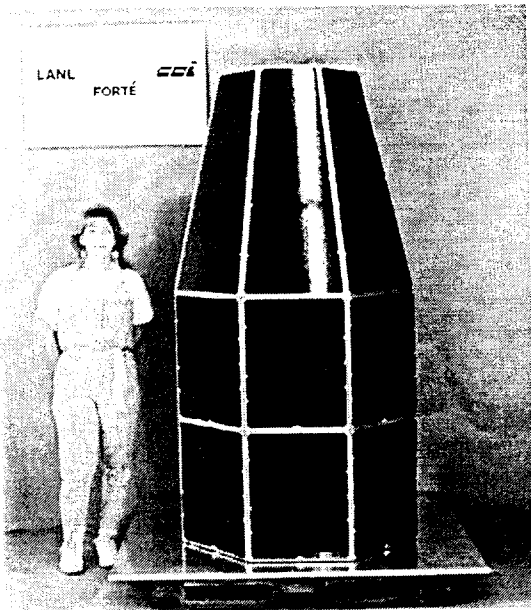
Figure 1. Fully assembled spacecraft structure with SAS panels installed
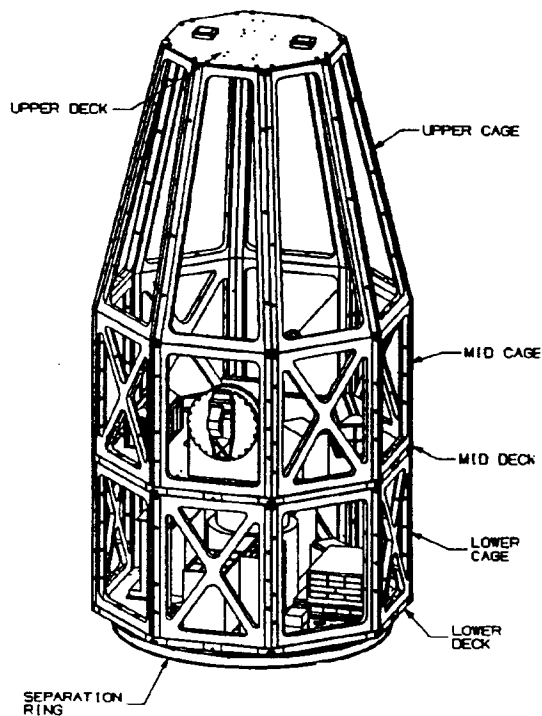

Figure 2. Structural components of the FORTÉ spacecraft

The three decks are termed the lower, mid and upper decks. The lower and mid decks are structurally identical to each other. Aluminum honeycomb core is sandwich-bonded between graphite/epoxy (Gr/E) skins. The upper deck closes out the structure and is fabricated from aluminum honeycomb sandwich-bonded between Gr/E skins.

The SAS panels are fabricated from the same materials as the upper deck. Aluminum inserts in the panels mate up against threaded block-type inserts in the cages. The substrates are then bolted into place.

The decks and cages are mechanically fastened to each other via aluminum corner fittings that are bonded into the cages and decks as shown in Figure 3. This arrangement ensures that the highly loaded structure has excellent load transfer in the corners of the cage.
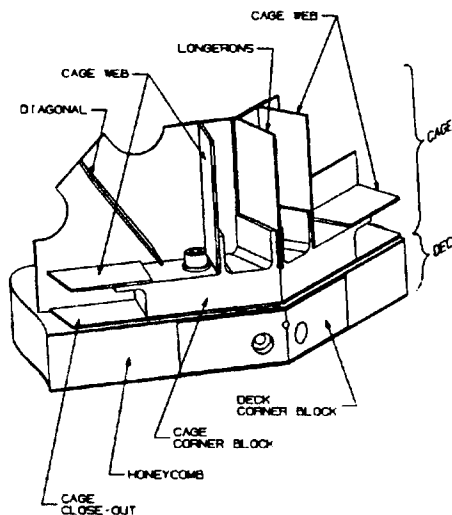

Figure 3. Spacecraft cage structure and deck joint detail with outer skin removed for clarity
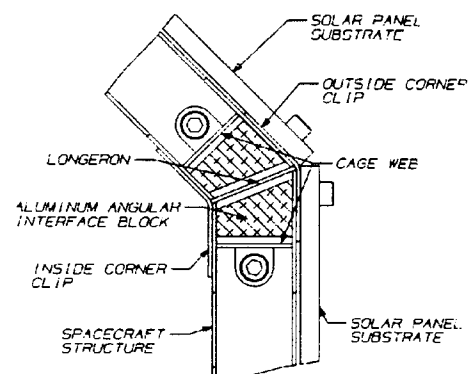

Figure 4. Cage structure joint detail

The cross-sectional view of the cage corner is shown in Figure 4. This view shows how the outer clip and inner clip are used to join the cage subassemblies together for a robust structural joint.

3. Design/Analysis Summary

The design of the FORTÉ spacecraft composite structure and solar panel substrates can best be discussed by addressing the following areas:

- structural design heritage
- design-to-cost considerations
- dynamic loads analysis
- structural analysis summary.

3.1. Structural Design Heritage

The premise for the FORTÉ design concept originated from earlier work LANL had done for the SSC. LANL designed an ultra stable support structure for the SSC GEM Silicon Tracker as shown in Figure 5. FORTÉ is using this concept again, keeping as many of the structural components similar to the original design to further reduce the cost of the structure. A corner detail can be seen in figure 6.

The original structural support consisted of an octagonal spaceframe made from advanced metal matrix composites (MMC). This network of tubes and joints proved to be highly stable and quite costly. The structure shown in Figure 5 was costed at one-tenth the comparable MMC frame cost, with only small degradation in stability. This large reduction in cost simply could not be overlooked in today's ever tightening budget scenario.
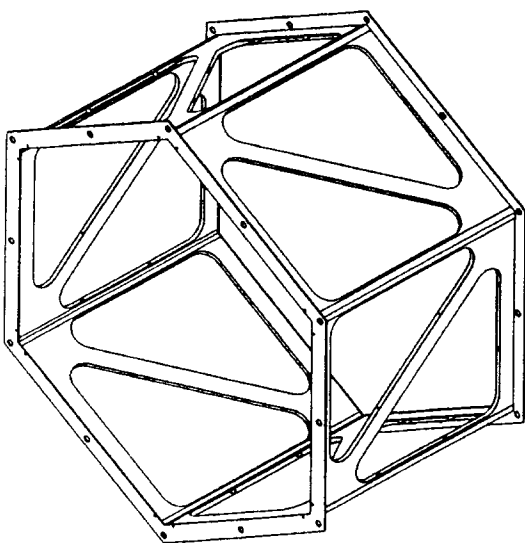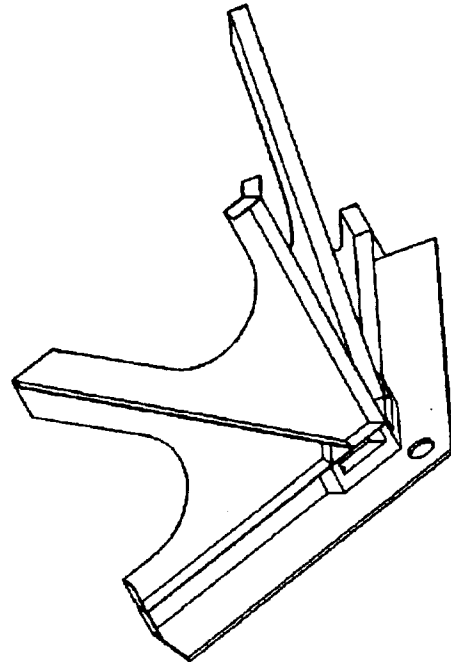

Figure 6. GEM tracker structure corner detail

Because of the apparent economic and structural benefits of this basic design approach for composite structures, engineers at LANL thought it prudent to replace the heavier aluminum design being considered for FORTÉ. LANL's subsequent structural analysis effort for FORTÉ was supported by an extensive material database that substantiated the suitability of this type of composite structural design concept. This will be evident in the following sections.

3.2. Design-to-Cost Considerations

A concept associated with composite structures is that they are much more expensive than aluminum structures. Technological advancements in the design and manufacturing of composite structures have disproved this idea. The cost of the FORTÉ spacecraft structure is very near that of the aluminum spacecraft structure it replaced. This was accomplished by using advanced design and manufacturing technology. For FORTÉ, the following design features were established to minimize manufacturing cost.

1. Design to maximize use of flat composite laminates to:
    - eliminate large production molds
    - increase the rate (pounds of prepreg per hour) at which composites can be laid up
    - minimize inspection time

Figure 5. GEM tracker structure

- facilitate use of programmable routers/waterjet machining
- reduce schedule by using existing composite stock material.
2. Design in commonalty between parts to:
    - minimize tooling
    - improve the learning curve (details and assembly)
    - allow laminate stacking for waterjet machining.
3. Design in self-fixturing techniques to:
    - minimize tooling
    - minimize subassembly time
    - minimize inspection time.

Along with these specific features that reduce the manufacturing cost comes a reduction in time needed to fabricate a unit. Time factors have a significant effect on the overall FORTÉ spacecraft program costs.

3.3. Dynamic Loads Analysis

Using the drop transient shock response spectrum for a Pegasus launch as a guide, the goal was to design the spacecraft structure so that the primary modal response would be at about 35 Hz. Preliminary analysis showed primary modes in the 20 Hz range with excessive deformation at the corners of the lower deck. Stiffeners added at the eight deck corners of the lower deck brought the primary modes up to the 50 Hz range. This is in the region of maximum response, which is not ideal, but is adequate. If the modal frequencies shift, any changes in frequency will lower these responses, which would be desirable.

A frequency analysis showed the first 19 modes to be between 35 Hz and 74 Hz. Several of the key vibrational modes are illustrated in Figures 7a and 7b.
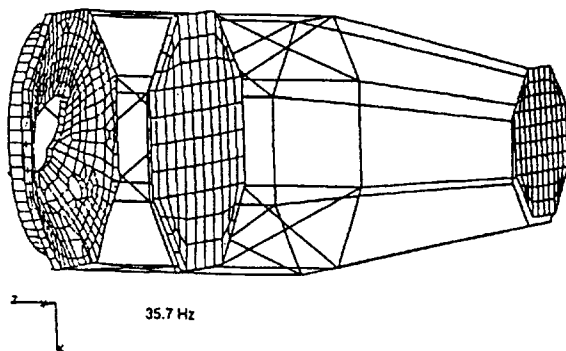

35.7 Hz

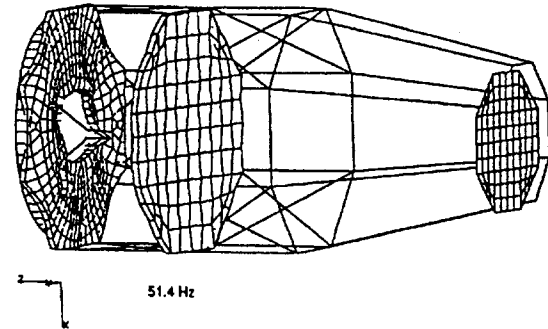**Figure 7a. First mode lower deck**

51.4 Hz

Figure 7b. First bending body mode Y-direction

3.4. Structural Analysis Summary

The analysis effort of the FORTÉ primary spacecraft structure focused on evaluating its performance and optimizing its design for the drop portion of the launch. The structure was also analyzed during the third stage acceleration but as noted earlier this was not the critical loading condition.

A finite element model (FEM) of the structure was constructed using the COSMOS\M finite element package. The structure was modeled using three-dimensional beam elements for the longerons that would make the backbone of the structure once the cages and decks were assembled. The decks were modeled using isotropic plate elements. The mechanical properties for the aluminum honeycomb graphite skin combination was calculated and used as input. To simulate the mass of the components on the decks, the mass was distributed uniformly over the surface. The SAS panels were modeled in an identical fashion. They were attached to the rest of the structure with short beam elements so that an estimate of the in-plane shear forces could be identified. The model was fixed at its base with spring elements to simulate the shock attenuating flexures.

The most severe acceleration that developed during the drop launch was a linearly varying lateral X-component acceleration of 8.5 g at the base and 18.5 g at the structure top deck. A constant lateral acceleration 2.5 g orthogonal to the linearly varying acceleration and a longitudinal acceleration of 4.5 g compressed the structure.

The initial design had no cross bracing in the cage structure and relied solely on the SAS panels to carrying the shear from the drop transient

accelerations. Analysis showed this arrangement was not feasible and studies were undertaken to determine the minimum number and location (acceptable to access requirements) of necessary cross bracing additions. In addition to the cross bracing, the number of fasteners in the substrates had to be increased from 6 per panel to 10 to meet the design allowable of 666 lbs shear-out for in-plane failure of the substrate. Figure 8 shows the component forces acting on a typical SAS panel while Table 1 shows the resultant loads.
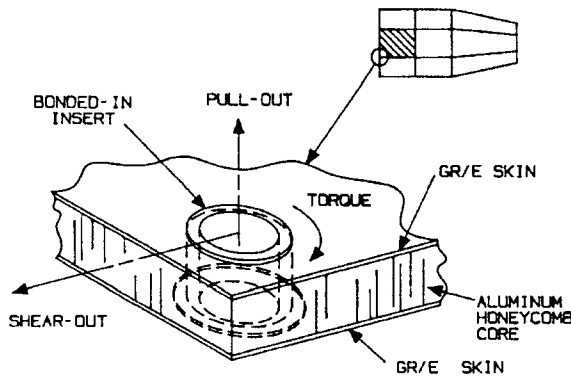

Figure 8. SAS panel showing maximum loads

Table 1: SAS Panel Resultant Loads

Load	Maximum Calculated	Allowable
Pull-Out	5 psi	516 psi
Shear-Out	265 lbs	666 lbs
Torque-Out	5 in-lbs	72.6 in-lbs

Forces from the beam elements were calculated and put into detailed model of the cage corner interface. A detailed FEM was made of the joint area to predict adhesive stresses. The results are summarized in Table 2 and Figure 9 illustrates the joint FEM.

Table 2: Joint Results

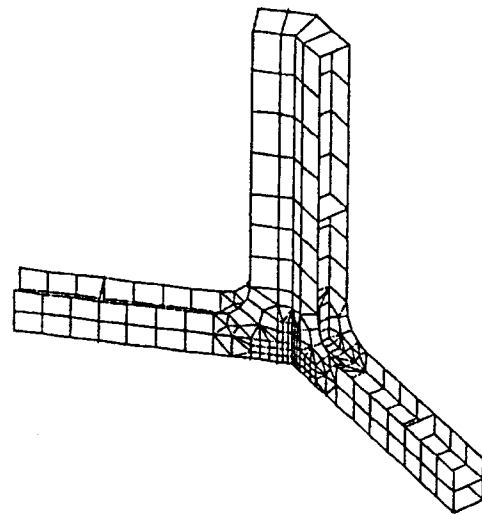| Longeron-Aluminum Block Max in Plane Shear Stresses	324 psi
Longeron-Aluminum Block Maximum Peel Stresses	517 psi
Maximum Outer Skin Von Mises Stress	2500 psi

Figure 9. FEM of the structural joint

The shear results in the SAS panels were then used to determine the buckling characteristics. The panel was analyzed using finite element and conventional composite techniques. To help gain confidence in the analytical results, modal testing was performed on the substrate panels. The first five natural frequencies were calculated using finite elements and then the panels actual first five frequencies were found. Table 3 shows the analytical modes compared to the measured values. Figure 10 shows the experimental mode shape for a Type A panel. The natural frequencies were found by subjecting the panels to sine sweep on the function and looking for peaks on the frequency response function (FRF). The panels were excited at frequencies close to the resonance and sand was used to identify the nodal points of the mode shape.

Table 3: Analytical and Measured Results for Fundamental Mode Shapes of Type A SAS Panel

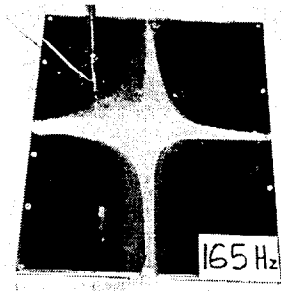| Mode #	FEM	FRF	% Difference
1	164.8	165	0.1%
2	203.3	214	5.0%
3	349.1	373	6.4%
4	375.5	389	3.5%
5	456.2	483	5.5%

Figure 10. Measured fundamental frequency of a Type A SAS panel

4. Fabrication

When bolted together the 3 frame structures, 3 equipment decks, and 24 SAS panels constitute the complete primary structure for the FORTÉ spacecraft, as shown previously in Figure 1. The following discussion addresses tooling and the various FORTÉ spacecraft structure components and illustrates the simple manufacturing approach afforded by this low cost structure.

4.1. SAS Panels

The 24 SAS panels for the upper, mid, and lower cages were fabricated and machined from 8 large panels that could produce 16 lower or mid panels and eight upper panels. The large panels were 0.020" thick precured panel assemblies of Gr/E T-50/ERL1962, [0/45/90/135]$_s$ with either co-cured 0.2 mil copper on one side or co-cured 2.0 mil Kapton®. Figure 11 shows a typical cross-section of an SAS panel.
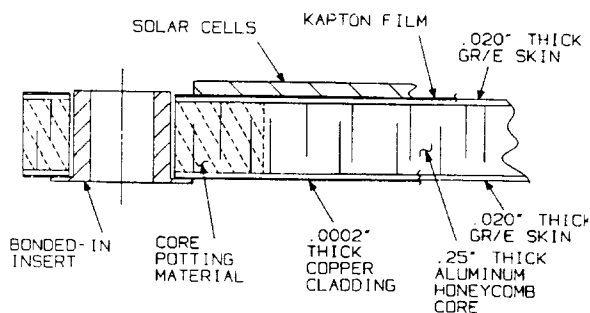

Figure 11. Typical cross section of an SAS panel

These precured skins were then bonded using FM-300-2U film adhesive to .25" aluminum honeycomb core (1/8" cell; 3.1 lbs/ft³). All aluminum inserts were post potted in Corefil 615 and bonded using room temperature epoxy adhesive, Hysol EA9394.

Insert locations were machined into the various panels at the time the sandwich subassemblies were cut from the larger panels. Then, using master bond plates that are common to those used for the corresponding frame subassemblies, all inserts were located into the SAS panel.

4.2. Spacecraft Structure

The space frame assemblies and equipment decks that make up the spacecraft structure differ in construction. The decks are manufactured similarly to the SAS panels, except that copper was co-cured on both sides of each deck. The space frame is made from flat laminates. The upper deck is the same thickness as the SAS panels but the mid and lower decks have a one inch thick aluminum core (1/8" cell, 4.3 lbs/ft³). Figure 12 shows a lower deck bonded and machined. The skin thickness on all decks is 0.030" with an orientation of [0/60/120]$_s$.
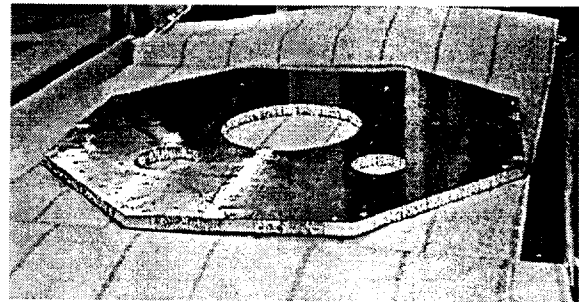

Figure 12. Lower deck

The frame subassemblies are made from flat 0.048" thick laminates of T50/ERL1962 with a [0/45/90/135]$_s$ orientation. As is typical of flat laminate construction, all details can be "nested" tightly on larger cured laminates and machined out with a waterjet machining head mounted to a programmable router. Four laminates of one configuration and two laminates of the other configuration were machined.

Utilizing COI's concept for a self-fixturing fabrication process (the Short Notice Accelerated Production Satellite or SNAPSAT™*), all details are removed from a completely processed panel (prepped for bonding) and "snapped" together. The snapping together feature is mortise and tenon joints that are precision machined into the details.

---

* SNAPSAT™ is a patent-pending trademark of COI.

Figure 13 shows a portion of the frame assembly. Note that blade longerons and inner and outer angle clips are not bonded at this time. The deck angular interface fittings are what initially ties the structure together. These are visible in Figure 14. Corner splicing angles are later installed which cover up the blade longeron. The upper and lower decks are used to assemble and jig the frame. Angular interface fittings accept the mid frame subassemblies. The frame assembly can then be bonded together on the decks.
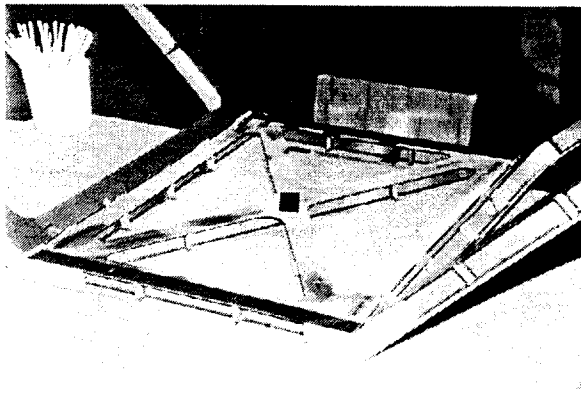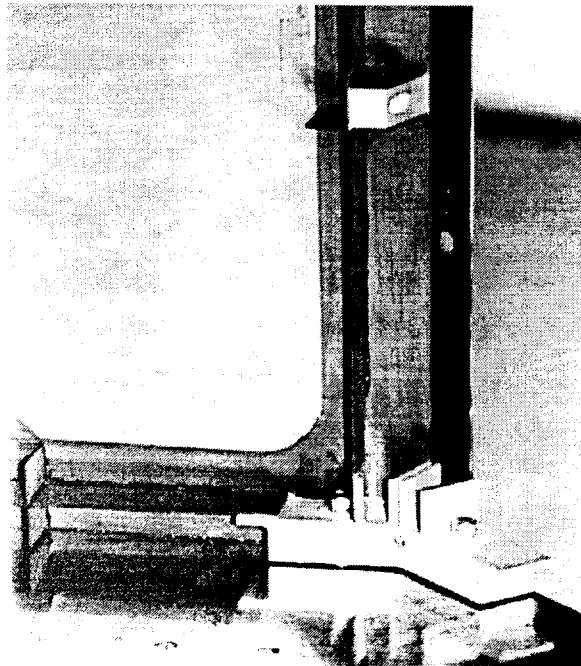
4.3. Final Assembly

By repeating the above process for all decks and frames, the final assembly shown in Figure 15 is achieved. The SAS panels have not yet been installed. Note that the mid and upper frame assemblies are unplated for this first unit. The lower frame assembly is copper electroplated plated on the outer surface of the outside panels only. This was done in order to evaluate the RF shielding effectiveness of unplated vs. plated Gr/E. Pending the electromagnetic interference (EMI) test results on the EM, the flight unit will be configured for EMI protection. The copper on the back of the SAS panels provides the EMI protection for the spacecraft equipment and also serves to electrically shield the spacecraft from its antenna system.
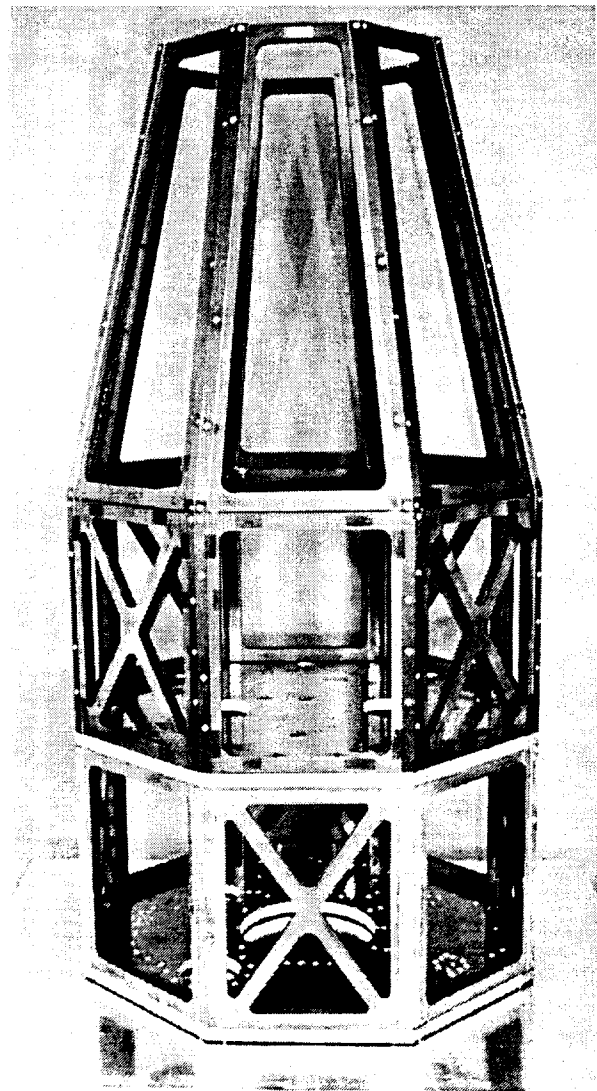

Figure 13. Cage panel frame subassembly showing the interface fittings

Figure 14. Cage corner detail

Figure 15. Final spacecraft assembly

5. Testing

5.1. Material Testing

The uniqueness of the FORTÉ primary spacecraft structure meant that some of the detailed design information was lacking. Parts of other spacecraft devices were similar but not exactly the same. A testing effort was initiated to define design allowables in critical areas. The primary concerns were the high shear stress areas of the SAS panels, the shear stress between the graphite and the aluminum angular interface block corner joints, and the deck component insert pullout allowables.

The SAS panels were viewed as the most critical area of the structure and no design data existed for them. Edge coupons were fabricated by COI, and tested at LANL. The coupons were designed to carry a maximum shear load through the corner of the coupon since analysis showed the maximum shear force was along this direction. Along with determining the absolute design allowables there was also an interest to know the effects of thermal cycling on the bonded joints.

The spacecraft would be maintained near room temperature during the launch phase, but it would be cycled from −65°C to 80°C five times prior to launch as part of its qualification testing. Therefore it would be imperative to know the effects of thermal cycling on the shear-out design allowable. Ten coupons were tested with thermal cycling and ten coupons were tested without thermal cycling. The cycle commenced at room temperature with the cooling to −65°C at a rate of 10°C/min. This extreme was held for 10 minutes and then the part was heated to 80°C at 10°C/min and held at that extreme for 10 minutes. Then the part was returned to room temperature. This cycle was repeated five times. All coupons were then tested at room temperature.

The results of the two tests are summarized in Table 4. The average ultimate shear-out load for the thermal cycled coupons degraded by 13% and the design allowable was decreased by 24%.

Ten additional coupons were tested after a modified thermal cycle. The extreme temperatures were held for one hour. The increased soak times at the extreme temperatures only decreased the mean ultimate shear-out load an additional 9% and the design allowable an additional 17%.

Table 4: Corner Static Load Test

	Mean Ultimate Shear-Out	Allowable Shear-Out
All Coupons Combined	940 lbs	750 lbs
Non Thermal Cycled Coupons	1003 lbs	881 lbs
Thermal Cycled Coupons	877 lbs	666 lbs

Another critical area for which little design data existed is the cage structure corners where aluminum angular interface blocks are bonded to the graphite skins. Initially the published shear strength for the adhesive was used to determine the design allowable. Fifteen single lap shear coupons were fabricated and tested at COI. Of the 15, 5 were not thermally cycled and 10 were subjected to the same thermal cycle as the corner coupons. The mean ultimate shear load showed no dependence on thermal cycling. The design allowables varied substantially, ranging from 507 psi for all 15, 473 psi for only the thermally cycled set, to 231 psi the non-thermal-cycled set. The very low value for the non-thermal-cycled set is a reflection of the small sample set size, given that the mean and standard deviation are almost identical to those of the other cases (Table 5).

Table 5: Shear Coupon Load Test

	Measured Bulk Area Mean Ultimate Shear Stress	Calculated Bulk Area Allowable Shear Stress
All Coupons Combined (15 Coupons)	895 psi	507 psi
Non-Thermal-Cycled (5 Coupons)	888 psi	231 psi
Thermal-Cycled (10 Coupons)	900 psi	438 psi

Analytical solutions and FEM's of the coupons were created to determine the stress distribution at failure. The analytical solution suggested by Ojalvo and Eidinoff, 1977 show a bulk shear stress of approximately 660 psi and a peak at the edge of the bond area of more than 5000 psi. Their results indicate a peak peel stress at the bond edge of 3550 psi. A plane two-dimensional model showed the same stress distributions as suggested by the analytical solutions but a bulk area shear stress of about 125 psi and a corresponding peak of 8600 psi.. In this case the stressesare plotted from the bonded joint center to the edge because of symmetry. The bulk area peel stress is initially close to zero, then becomes compressive near the edge and peaks at the very edge at almost 13,500 psi when the peel stress is plotted against the bonded joint length.

The actual joint in the FORTÉ structure unfortunately does not resemble the lap shear coupons. In the structure a relatively thin graphite skin is bonded to a relatively massive aluminum block (Figure 3). Therefore, further study of the lap shear finite element model was done to determine the effect of considerably increasing the thickness of one adherent on the stress distribution. The results showed a dramatic change in both the shear and peel stresses. The bulk area shear stress was reduced slightly to 580 psi. The shear stress then peaks at the bond edge at slightly over 3800 psi. The bulk area peel stress is initially 170 psi and increases to 435 psi. The peel stress then peaks at the bond edge at–2227 psi. These results indicate that the peel stress is reduced significantly when one adherent is much thicker than the adhesive and the other adherent.

The results also show that the bulk area shear stresses are lower than those determined from the lap shear coupons tests (indicated in Table 5). To determine those values the ultimate load was divided by the bond area. From the FEM shown in Figure 9, the maximum shear stress calculated was 324 psi and the peak peel stress was 517 psi, far below the analytical results or the finite element predictions. These are slightly larger than the allowables determined by testing, but when compared to the analytical results or the FEMs the peak stresses may be considered acceptable.

6. Conclusions

LANL has designed, analyzed, and demonstrated a simplified, cost-effective method for the production of small satellite spacecraft structures, which can be readily applied to stable structure design. This process produces an all-composite spacecraft structure that is lightweight and very strong, providing substantial improvement over aluminum designs in its payload-to-weight ratio. The fabrication technology that has been developed produces savings in production time and expense over previous composite processes. It is competitive with aluminum structure processes in expense and speed of production and is applicable to a wide variety of stable structures. The simple but robust spacecraft structure provides a platform that will be useful for a wide variety of scientific applications.

7. References

"GEM Silicon Tracker Mechanical Subsystem Final Design Report", Los Alamos National Laboratory, June 1994.

Goland, M. and E. Reissner, "The Stresses in Cemented Joints", Journal of Applied Mechanics, March 1994, Vol. 11, pp. A17-A27.

Griiffin, M. D. and J. R. French, *Space Vehicle Design*, AIAA Publishing, 1991, pp. 345, 351, 356.

"Mechanical Properties of Hexcel Honeycomb Materials", Hexcel TSB 120, Hexcel Corporation, 1987.

"Guidelines for the Presentation of Data", MIL-HDBK-5D, June 1, 1983.

Kilpatrick, M., J. Girard, K. Dodson, "Design of a Precise and Stable Telescope Structure for the Ultraviolet Chronograph Spectrometer (UVCS)", SPIE, Volume 1690, Design of Optical Instruments, 1962.

Ojalvo, I.U., and H. L. Eidinoff, "Bond Thickness Effects Upon Stresses in Single-Lap Adhesive Joints", AIAA Journal, Vol.16, No.3, 1977.

Pegasus Air Force Small Launch Vehicle Interface Design Document, Release 1.00, August 31, 1993.